Fabrication and electrical characteristics of carbon nanotube-based microcathodes for use in a parallel electron-beam lithography system

K. B. K. Teo,[a] M. Chhowalla, G. A. J. Amaratunga, and W. I. Milne
Department of Engineering, University of Cambridge, Trunpington Street, Cambridge CB2 1PZ, United Kingdom

P. Legagneux, G. Pirio, L. Gangloff, and D. Pribat
Thales Research and Technology, Domaine de Corbeville, 91404 Orsay Cedex, France

V. Semet and Vu Thien Binh
Laboratoire d'Emission Electronique, DPM-CNRS, Université Lyon 1, Villeurbanne 69622, France

W. H. Bruenger, J. Eichholz, H. Hanssen, and D. Friedrich
Fraunhofer Institut ISiT, Germany

S. B. Lee, D. G. Hasko, and H. Ahmed
Microelectronics Research Centre, Cavendish Laboratory, University of Cambridge Madingley Road, Cambridge CB3 0HE, United Kingdom

(Received 28 May 2002; accepted 16 December 2002; published 12 February 2003)

This article presents an overview of the ''*Nanolith*'' parallel electron-beam (e-beam) lithography approach. The e-beam writing head consists of an array of microguns independently driven by an active matrix complementary metal–oxide–semiconductor circuit. At the heart of each microgun is a field-emission microcathode comprised of an extraction gate and vertical carbon nanotube emitter, whose mutual alignment is critical in order to achieve highly focused electron beams. Thus, in this work, a single-mask, self-aligned technique is developed to pattern the extraction gate, insulator, and nanotubes in the microcathode. The microcathode examined here (150×150 gates, 2 μm gate diameter, with multiple nanotubes per gate) exhibited a peak current of 10.5 μA at 48 V when operated with a duty cycle of 0.5%. The self-aligned process was extended to demonstrate the fabrication of single nanotube-based microcathodes with submicron gates. [DOI: 10.1116/1.1545755]

I. INTRODUCTION

The 2001 International Technology Roadmap for Semiconductors (2001 ITRS) and the European Commission Technology Roadmap for Nanoelectronics (2000 TRN) favor the deep/extreme UV (DUV/EUV) approach for lithography at 90 nm feature size and below. Nevertheless, electron-beam (e-beam) direct write (EBDW) techniques are still considered as potential candidates because sub-100 nm beam sizes are ''easily'' obtained. The drawback associated with EBDW is the low throughput due to serial writing. To solve this problem, a relatively straightforward concept is to use an array of parallel electron beams. The feasibility of this approach has been demonstrated by Chang *et al.*[1] and Muray *et al.*[2] using an array of four miniature (2×2 cm) e-beam columns. To further reduce the size of each column to submillimeter range, Binh *et al.*[3] studied the concept of the microgun which used a nanotip in tandem with micron-sized electrostatic extraction, focus, and deflection optics fabricated on a single silicon substrate to obtain nanometric spot-sized electron beams. ''*Nanolith*'' is an European IST project which investigates the feasibility of parallel e-beam lithography, with the initial aim of demonstrating the concept with 32 microguns. The long-term ambitious objective is to achieve high throughput maskless direct writing capability with an array of 1 million microguns. Even if the throughput of EBDW does not reach the levels of DUV/EUV in the near future, parallel e-beam lithography could still find itself suitably poised for low cost photomask fabrication (since low throughput single e-beam systems are currently used for manufacturing photomasks) and economical low volume maskless prototype circuit fabrication [as a set of photomasks for current complementary metal–oxide–semiconductor (CMOS) circuits costs 2 million Euros].

II. WRITING HEAD DESIGN AND EXPOSURE STRATEGY

In the *Nanolith* approach, the microgun integrates the carbon nanotube (CNT)-based electron source with the extraction and focusing optics, but does not include deflection capabilities [Fig. 1(a)]. Consequently, in order to address all the ''pixels'' in a writing field, the e-beam writing head (or the sample) needs to be scanned using a piezodriven stage with a control system determining the required pixels to be exposed [Fig. 1(b)]. This fixed-focus/fixed-position e-beam approach has the advantage that the lenses are simpler to design because it eliminates the aberrations associated with beam deflection (e.g., pincushion distortion). Thus, if the microguns have a pitch of 100 μm, the writing time for an entire mask would be the time to scan only the 100 μm$\times$100 μm field.

[a]Author to whom correspondence should be addressed; electronic mail: kbkt2@eng.cam.ac.uk

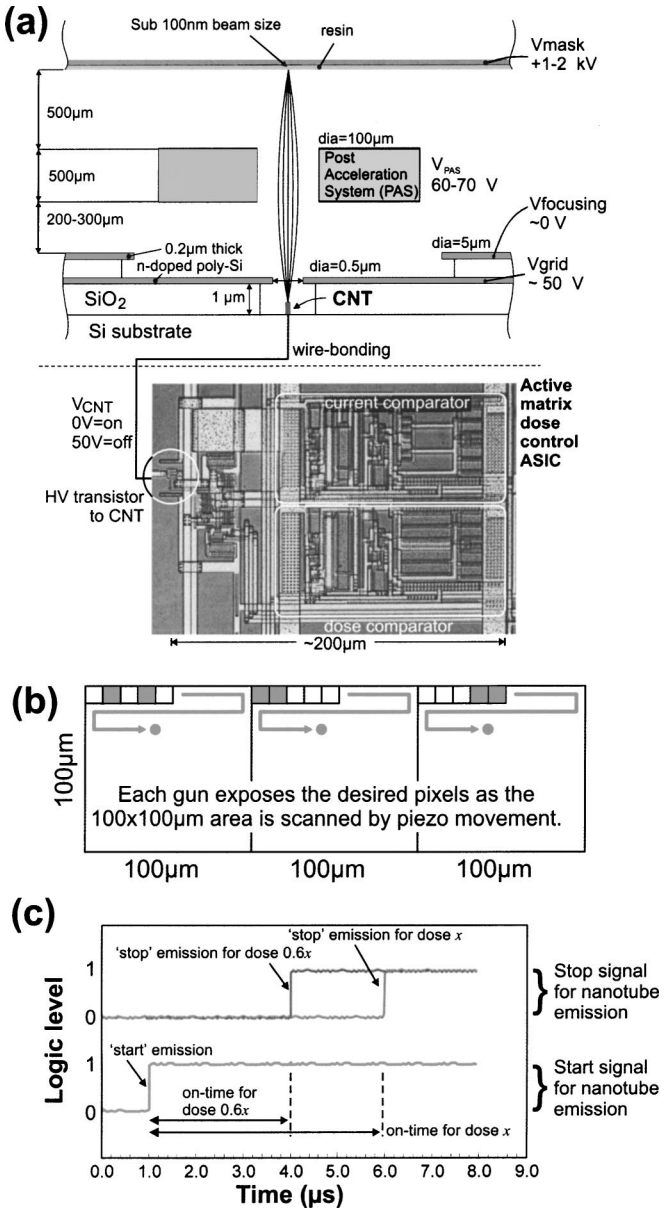

FIG. 1. (a) Design of one element of the *Nanolith* writing head. The fixed-focus/fixed-position microgun contains a CNT emitter, extraction grid/gate, focus electrode, and PAS lens. The CNT is electrically connected to an active matrix circuit (fabricated from 0.8 μm 80 V CMOS) which monitors the emission current and controls the dose delivered to expose each pixel. (b) The resist exposure strategy for an array of electron beams spaced 100 μm apart. (c) The dose control circuits have been verified using a dummy emission load of 10 nA. Two arbitrary doses (one 60% of the other) were set and the circuit modulated the on time of the emission current to deliver the correct charge/dose.

The goal is to achieve a writing time in the order of 1–5 min. For nonchemically amplified poly(methylmethacrylate) (PMMA)-based e-beam resist (e.g., Merck PMMA, Selectilux EB 250 A) which has a sensitivity of 2–40 μC/cm^2 for 1–3 keV electrons (since the resin potential is at 1–2 kV), this corresponds to a current of 3.3–67 pA per microgun at the minimum exposure window of 1 min. Note that if the writing head was used to scan over 200 μm$\times$200 μm, four microguns would cover each 100 μm$\times$100 μm field. This provides redundancy in case of gun failure or insufficient dose delivered by a gun.

Figure 1(a) schematically shows a single element of the writing head, which includes the microgun, the independent CMOS drive circuits and a postacceleration system (PAS). The PAS electrically screens the low-voltage microgun from the high acceleration voltage and also physically shields the microgun from back ion bombardment due to the outgassing of the resist during exposure. As variations in microgun current are expected due to fabrication irregularities, the use of active matrix CMOS circuits to control the delivered electron dose to expose the resist is vital in our approach. If each microgun has current which is sufficiently large to expose the resist, the on-time of the emitter could be modulated to deliver the intended dose. We have fabricated and tested circuits which can control the dose for emission currents of $\leqslant$10 nA (this upper current limit is due to very short on-time/switching speed limits). The circuits operate by integrating the emission current with time, and hence a specific dose could also be used as an input into the system. The switching wave forms of an active matrix circuit are shown in Fig. 1(c). Here, a constant current of 10 nA (via a dummy load) was used to test the circuit, and two different dose values were input. The circuit modulated the on-time (signified by the ''start'' and ''stop'' digital wave forms) of the current to deliver the chosen dose. Similarly, if two different currents were used for a fixed dose, the circuit would respond in the same way by initiating the stop pulse at the correct time.

Our preliminary simulations of electron trajectories show that the microgun structure (for the dimensions given in Fig. 1) leads to a spot size of about 30 nm for a 30 nm diameter CNT. However, the most critical parameter for obtaining this resolution is the alignment between the CNT and the extraction gate hole. The misalignment from the central axis must be below 50 nm to obtain sub-100 nm resolution if we assume that the semiangle of the beam at the CNT apex is 10°. This assumption comes from other experiments where we have observed emission spots with a beam opening of typically $+/-10°$ using a phosphor screen. This led to the development of a self-aligned fabrication process between the CNT emitter and extraction gate (i.e., the ''microcathode''), which will be discussed in this article.

III. CARBON NANOTUBE/NANOFIBER ELECTRON SOURCE

It has recently been demonstrated that CNT's/nanofibers/nanocones can be deposited with a high degree of control over their alignment, height, and diameter using catalytic plasma enhanced chemical vapor deposition (PECVD).[4–6] The deposition process employed here[7] is shown in Fig. 2(a). A thin film of Ni catalyst was prepared by sputtering and patterned on a substrate surface with a thin diffusion barrier layer, typically insulating SiO_2 or conductive TiN. In step 1, the substrate was heated to 700 °C and the Ni film formed nanoclusters, followed by step 2 which is CNT growth by PECVD in the presence of acetylene and ammonia gases at

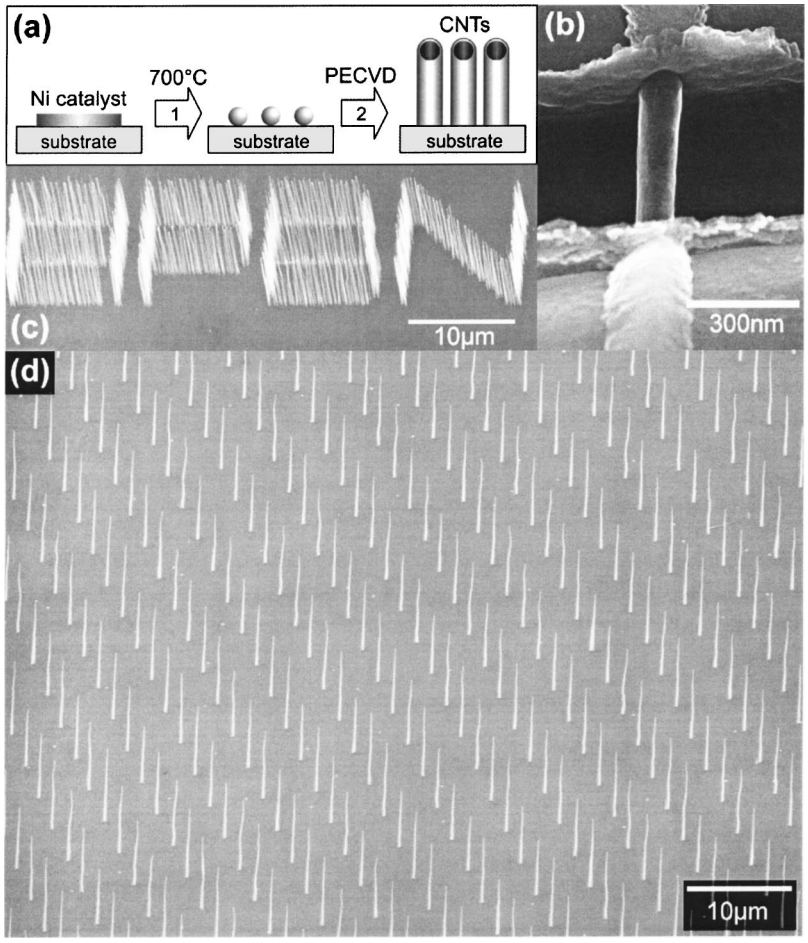

FIG. 2. (a) CNT growth process. (b) Nanotubes were suspended between Nb contacts for electrical conductivity measurements (SEM tilt 40°). (c) The initials of the conference title, EIPBN, were written in nanotubes by prepatterning the Ni catalyst (SEM tilt 45°). (d) Uniform arrays of single CNT's fabricated using 100 nm patterned catalyst dots (SEM tilt 55°).

700 °C. In direct contact measurements of PECVD nanotube bridges [e.g., Fig. 2(b)], we found that the nanotubes are highly conductive in nature. In a typical measurement, a 55 nm diameter nanotube could carry 2 mA ($J \sim 10^8$ A/cm^2) with a resistance of 1 kΩ per μm length. By prepatterning the Ni catalyst prior to growth, patterned arrays of nanotubes [Fig. 2(c)] or even individual vertically oriented CNT's [Fig. 2(d)] could be deposited with great uniformity. For instance, the standard deviation in the tip diameter and height were found to be 4.1% and 6.3%, respectively, for the growth of individual CNT's.[8] Recently, Baylor *et al.*[9] reported the emission from individual PECVD carbon nanocones and found favorable emission properties as expected from the high aspect ratio of the structures. In our recent work, we have additionally found that the emission characteristics between various CNT's in an array, after conditioning, are quite uniform ($\Delta I/I = 30\%$) and they could carry high emission currents of 20 μA.[10]

IV. FABRICATION AND ELECTRICAL CHARACTERISTICS OF A CARBON NANOTUBE MICROCATHODE

Recently, Guillorn *et al.*[11] demonstrated the operation of a gated microcathode using a single conical carbon nanofiber emitter. In their fabrication process, manual alignment was used between the extraction gate and the emitter. Due to the high degree of alignment required between the extraction gate and CNT from our simulations, we developed a self-aligned fabrication process instead. Compared to manual alignment, a self-aligned process is potentially advantageous when applied to a large area/number of microguns simultaneously. Furthermore, the alignment becomes increasingly difficult for manual techniques when submicron gate holes are used, whereas self-alignment overcomes this issue.

Our process[12] starts with the deposition of a sandwich structure comprising of: 150 nm *n*-doped polysilicon (extraction gate electrode); 500 nm silicon dioxide (insulator); TiW/Mo/TiW (emitter electrode); and oxidized silicon substrate. An array of holes was then patterned over a 600 μm$\times$600 μm area (150$\times$150 holes of 1 μm diameter with a pitch of 4 μm), see Fig. 3(a). A reactive ion etching step using SF_6 gas was then used to isotropically etch the polysilicon gate. Wet chemical etching in buffered hydrofluoric acid was used to isotropically etch the silicon dioxide insulator. Both the gate and insulator were deliberately overetched to produce an undercut profile, shown schematically in Fig. 3(b) and in scanning electron microscopy (SEM) cross section in Fig. 4(a). A 20 nm thick TiN layer was then deposited by sputtering. This was followed by evaporation of 3 nm of Ni, which is the catalyst for CNT growth [Fig. 3(c)]. The role of the TiN layer is to prevent Ni diffusion into the TiW/Mo/TiW electrode during the CNT growth at 700 °C. The un-

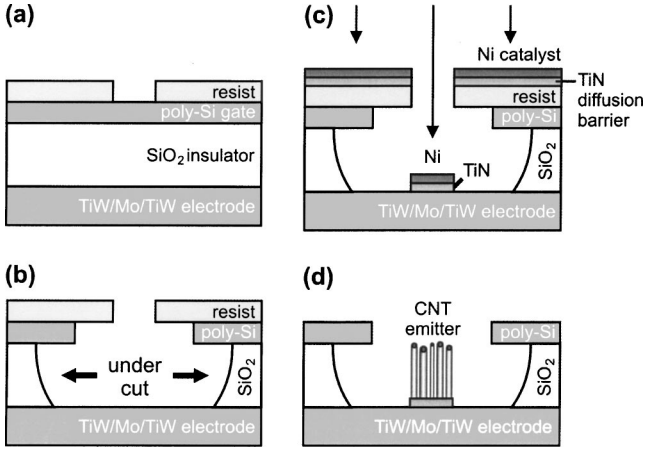

FIG. 3. Self-aligned process for fabricating nanotube-based microcathodes. (a) Definition of holes in resist, (b) etching of the poly-Si gate and SiO_2 insulator, (c) deposition of the TiN diffusion barrier and Ni catalyst, and (d) lift off of resist and nanotube growth by PECVD.

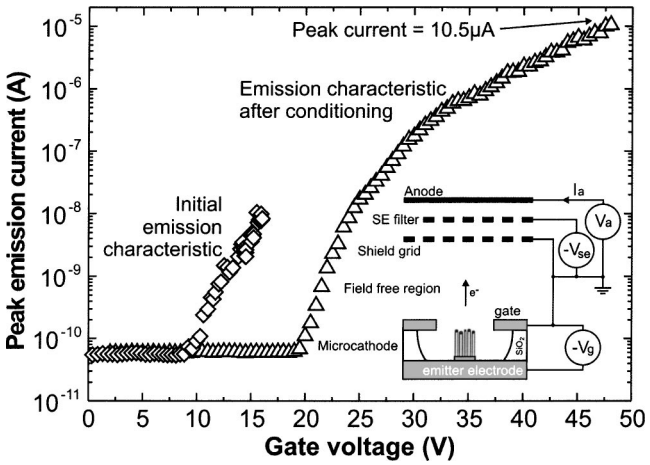

FIG. 5. Peak emission current (I_a) as a function of the applied gate voltage (V_g) at 0.5% duty cycle. Emission characteristics from the as-prepared microcathode (initial emission) and after conditioning are shown. The inset shows the measurement setup for this experiment.

wanted TiN and Ni over the gate were then removed by lift off. The vertically aligned CNT's were deposited using PECVD with acetylene and ammonia gases at 700 °C [Fig. 3(d)]. The average height of the nanotubes was controlled by the deposition time (2 min) to be 0.5 μm, which was equal to the insulator height. For a 1 μm diameter catalyst area, multiple nanotubes were obtained at each gate, as shown in the SEM pictures of Figs. 4(b)–4(d). It is clearly evident from the top view image of the microcathode [Fig. 4(c)] that the nanotubes were centrally located with respect to the gate aperture. Note that the nanotubes were grown in a 1 μm diameter circle, which was defined by the initial 1 μm diameter resist hole, whereas the polysilicon (poly-Si) gate aperture was much larger (2 μm diameter) due to the isotropic overetching of the gate under the resist hole. The larger gate diameter ensured that short circuits between the gate and the nanotubes were eliminated.

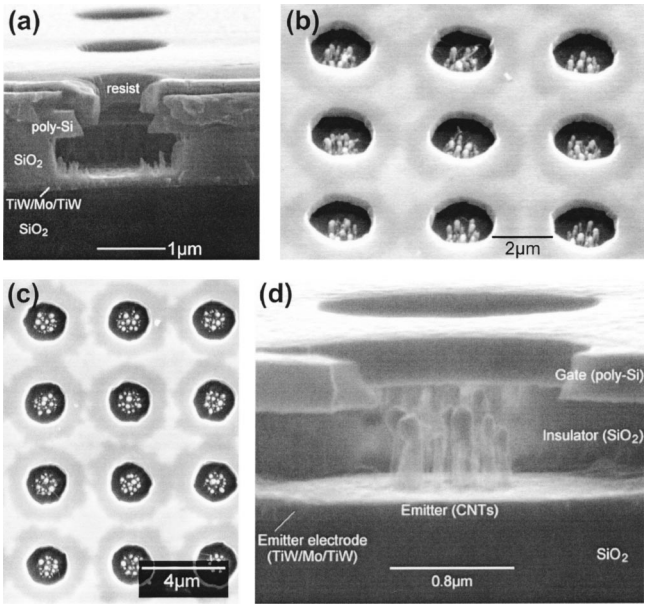

FIG. 4. (a) Cross section SEM showing the undercut of the poly-Si and SiO_2 beneath the resist. (b) Tilted 45° view of the microcathode after nanotube growth. (c) Top view clearly shows the centrally located nanotubes (bright dots) with respect to the gate hole. (d) Cross section SEM of the microcathode.

There was also a height and diameter distribution in the nanotubes as seen in the cross section SEM of Fig. 4(d). This was due to the random formation of catalyst nanoclusters from the "large" (1 μm) catalyst, and better uniformity is possible when high-resolution lithography is used to define the catalyst such that a single catalyst nanocluster is formed as shown in Fig. 2(d).[8]

After CNT growth, this microcathode was tested using the measurement configuration shown in the inset of Fig. 5. Either dc or a square wave voltage (V_g) was applied between the gate and the emitter of the microcathode. Pulse mode operation allows high peak emission currents to be extracted while limiting the overall power, which prevents the degradation of the device. The field-emitted electrons were then filtered to remove low-energy secondary electrons (e.g., generated by bombardment of the gate) by biasing the filter grid, V_{se}, at a small negative voltage (about -10 V). The anode was biased at $+80$ V (V_a) to collect and measure the emitted electron current (I_a). The measurement results shown in Fig. 5 were performed with a duty cycle of 0.5% and a frequency of 100 Hz. The initial turn-on voltage (voltage required to produce detectable emission) was 9 V. After conditioning by cycling the gate voltage, a peak emission current of 10.5 μA was obtained at 48 V gate voltage. It is necessary to initially condition these nanotube emitters as this process drives off the adsorbates (due to air exposure of the microcathode) on the nanotube tips to yield stable emission characteristics with higher current, as discussed in Ref. 10. Assuming that every gated aperture is emitting, the average current per aperture was 0.5 nA at 48 V.

Recently, using the self-aligned technique with a 200 nm resist hole, we have produced single CNT microcathodes

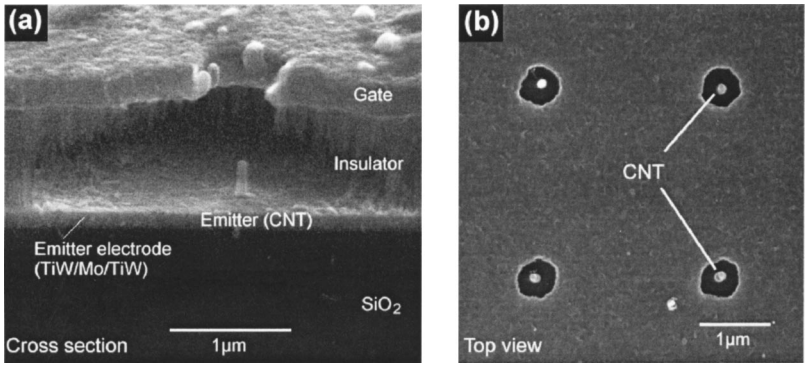

FIG. 6. Tilted (a) and top view (b) of a single nanotube based microcathode, showing the validity of the self-aligned process for smaller gate holes and single emitters.

(see Fig. 6) with the desirable grid and emitter dimensions corresponding to the schematic of Fig. 1(a). Note that in the self-aligned process, both the TiN diffusion barrier (under the catalyst) and the Ni catalyst are patterned simultaneously. Thus, as the nanotube can only be formed on the diffusion barrier (any Ni outside the TiN area will alloy with Ti/W electrode which yields no nanotube growth), this means that the nanotube will essentially be confined within the patterned diffusion barrier. Since we used a 200 nm diameter resist hole here, the maximum misalignment within the diffusion barrier area is thus $+/-100$ nm. If 100 nm lithography is used to define the diffusion barrier and the catalyst, then the misalignment becomes smaller, i.e., $+/-50$ nm. We believe the actual gate will still be self-aligned with respect to the diffusion barrier area as it is isotropically overetched from the same defining lithographic step in the fabrication process. Therefore, the maximum misalignment is predicted to be $+/-50\%$ the resolution used to define the diffusion barrier and the catalyst. These microcathodes are currently under test and the emission results will be reported in the future.

V. CONCLUSION

An overview of the development of the *Nanolith* parallel e-beam writing head has been described in this article. Highly controlled deposition of conductive CNT's can be achieved using PECVD. Due to the stringent alignment requirement between the emitter and the extraction gate for beam focusing, a self-aligned fabrication process for the extraction gates and the CNT emitters was developed. The average current per gate aperture was found to be 0.5 nA which is in excess of the minimum current required for exposing the resist. The on time of the emission is modulated with active matrix circuits in order to deliver the correct dose. Work is currently in progress on the integration of the various parts of the writing head, namely the dose control circuit, the microcathode and lenses (microgun), and piezodriven stage and control system, for a 32 microgun demonstrator of the *Nanolith* concept.

ACKNOWLEDGMENTS

This work was funded by the European Commission through the IST-FET project *Nanolith*. One of the authors (K.B.K.T.) acknowledges the support of the Association of Commonwealth Universities and the British Council.

[1]T. H. P. Chang, D. P. Kern, and L. P. Muray, J. Vac. Sci. Technol. B **10**, 2743 (1992).
[2]L. P. Muray, J. P. Spallas, C. Stebler, K. Lee, M. Mankos, Y. Hsu, M. Gmur, and T. H. P. Chang, J. Vac. Sci. Technol. B **18**, 3099 (2000).
[3]V. T. Binh, V. Semet, D. Guillot, P. Legagueux, and D. Pribat, Appl. Phys. Lett. **73**, 2048 (1998); A. Zlatkin and N. Garcia, *ibid.* **75**, 1807 (1999).
[4]Z. F. Ren, Z. P. Huang, J. W. Xu, J. H. Wang, P. Bush, M. P. Siegal, and P. N. Provencio, Science **282**, 1105 (1998); Z. F. Ren, Z. P. Huang, D. Z. Wang, J. G. Wen, J. W. Xu, J. H. Wang, L. E. Calvet, J. Chen, J. F. Klemic, and M. A. Reed, Appl. Phys. Lett. **75**, 1086 (1999).
[5]V. I. Merkulov, D. H. Lowndes, Y. Y. Wei, G. Eres, and E. Voelkl, Appl. Phys. Lett. **76**, 3555 (2000).
[6]K. B. K. Teo, M. Chhowalla, G. A. J. Amaratunga, W. I. Milne, D. G. Hasko, G. Pirio, P. Legagneux, F. Wyczisk, and D. Pribat, Appl. Phys. Lett. **79**, 1534 (2001).
[7]M. Chhowalla, K. B. K. Teo, C. Ducati, N. L. Rupesinghe, G. A. J. Amaratunga, A. C. Ferrari, D. Roy, J. Robertson, and W. I. Milne, J. Appl. Phys. **90**, 5308 (2001).
[8]K. B. K. Teo *et al.*, Nanotechnology **14**, 204 (2003).
[9]L. R. Baylor, V. I. Merkulov, E. D. Ellis, M. A. Guillorn, D. H. Lowndes, A. V. Melechko, M. L. Simpson, and J. H. Whealton, J. Appl. Phys. **91**, 7 (2002).
[10]V. Semet, V. T. Binh, P. Vincent, D. Guillot, K. B. K. Teo, M. Chhowalla, G. A. J. Amaratunga, W. I. Milne, P. Legagneux, and D. Pribat, Appl. Phys. Lett. **81**, 343 (2002).
[11]M. A. Guillorn, A. V. Melechko, V. I. Merkulov, E. D. Ellis, C. L. Britton, M. L. Simpson, and D. H. Lowndes, Appl. Phys. Lett. **79**, 3506 (2001).
[12]G. Pirio, P. Legagneux, D. Pribat, K. B. K. Teo, M. Chhowalla, G. A. J. Amaratunga, and W. I. Milne, Nanotechnology **13**, 1 (2002).